*Journal of The Electrochemical Society*, **157** (6) B852-B855 (2010)
0013-4651/2010/157(6)/B852/4/$28.00 © The Electrochemical Society

# Steam Electrolysis Using a Microtubular Solid Oxide Fuel Cell

**M. A. Laguna-Bercero,[a,b,z,*] R. Campana,[a] A. Larrea,[a,*] J. A. Kilner,[b,*] and V. M. Orera[a]**

[a]*Instituto de Ciencia de Materiales de Aragón, Consejo Superior de Investigaciones Científicas–Universidad de Zaragoza, 50009 Zaragoza, Spain*
[b]*Department of Materials, Imperial College London, SW7 2AZ London, United Kingdom*

Reversible operation of a microtubular solid oxide fuel cell (SOFC) with high electrochemical efficiency is reported. These devices can ideally produce hydrogen from electricity and steam [solid oxide electrolyser (SOE)] and then use the stored hydrogen to generate electricity and heat (SOFC), acting as a storage device for the electrical energy. A fuel-electrode-supported Ni–yttria-stabilized zirconia (YSZ)/YSZ/$(La_{0.8}Sr_{0.2})_{0.98}MnO_3$ cell, 2.4 mm in diameter and 20 μm of electrolyte thickness, was evaluated in an electrolysis mode as a function of the steam concentration supplied to the Ni/YSZ electrode. A good cell performance was obtained at temperatures as high as 950°C for the electrolysis operation. At 850°C, the cell withstood current densities of $-1$ A/cm$^2$ at 1.3 V with steam utilization of 16.5%. The production of hydrogen in the electrolyzer was tested by mass spectrometry. Their performance, especially in the SOE mode, is very promising for high temperature electrolysis applications. Voltage–current curves present an S-shaped nonlinear behavior in the electrolysis mode with a tendency to saturate at high current density values. The cell could sustain current densities as high as $-6$ A/cm$^2$ at 1.5 V, using 70% $H_2O$/15% $H_2$/15% $N_2$ as a fuel with an area-specific resistance of the cell of 0.26 Ω cm$^2$. The origin of this effect is discussed.
 [DOI: 10.1149/1.3332832] 

Manuscript submitted October 27, 2009; revised manuscript received February 1, 2010. Published April 23, 2010. This was Paper 1460 presented at the Vienna, Austria, Meeting of the Society, October 4–9, 2009.

Hydrogen is a promising candidate as a clean fuel for the future. One of the critical barriers in research related to future energy sources is the production, storage, and distribution of hydrogen. For example, in the transportation sector, there is a wide number of refuelling stations for fuel cell vehicles requiring an on-site hydrogen production. At present, hydrogen is mainly produced from reforming of fossil fuels; however, carbon emissions to the atmosphere should be avoided in a large-scale production. Other cleaner methods include biomass, water electrolysis, biological systems, and the use of thermochemical cycles. All these are competing as future alternative methods to gas reforming, but probably the most advanced nowadays is the generation of hydrogen by electrolysis of water, a technology widely developed at low temperature using alkaline electrolysers. One of the advantages of using high temperature solid oxide electrolysis cells (SOECs) instead of the low temperature devices is that the electrical energy demand is significantly reduced.[1] The total energy demand ($\Delta H$) for water and steam decomposition is defined as the sum of the Gibbs energy ($\Delta G$) and the heat energy ($T\Delta S$), according to Eq. 1

$$\Delta H = \Delta G + T\Delta S \quad [1]$$

The electrical energy demand $\Delta G$ decreases with increasing temperature. For example, the ratio of $\Delta G$ to $\Delta H$ is about 93% at 100°C and about 70% at 1000°C. In addition, the high temperature helps in increasing the reaction kinetics and reducing the cathodic and anodic overvoltages, which cause some loss of power in electrolysis. According to the studies of Jensen et al.,[2] the solid oxide electrolyzer (SOE) technology has the capability to produce fuel from renewable energy sources or to utilize the excess energy from existing power stations. Thus, the SOE can produce hydrogen with lower electric power than the conventional water electrolysis.

The electrochemical reactions that take part in an SOE are the inverse reactions to that in a solid oxide fuel cell (SOFC). Cell polarization is the opposite, and anode and cathode interchange their roles. In an SOE, water acts as a reactant, and it is supplied to the cathode side of the cell (anode electrode in the SOFC mode). Oxygen ions are transported to the anode through the electrolyte, and hydrogen is produced at the cathode side. The reactions in the cathode and anode are

$$H_2O + 2e^- \rightarrow H_2(g) + O^{2-} \quad \text{(cathode)} \quad [2]$$

$$O^{2-} \rightarrow \tfrac{1}{2}O_2(g) + 2e^- \quad \text{(anode)} \quad [3]$$

Another advantage of SOEs is that they could operate reversibly as an SOFC-producing electricity with high efficiency. These devices can produce hydrogen from steam (SOE mode) and then use the stored hydrogen to generate electricity and heat (SOFC mode), acting as a storage device for electrical energy. Apart from the steam electrolysis, SOECs offer a wide range of possible applications, including $CO_2$ electrolysis,[3] coelectrolysis of steam, and $CO_2$,[4] or natural gas-assisted electrolysis;[5,6] even so most recent work is focused on steam electrolysis.[7-11] One of the problems of operating at high temperatures is the durability of the cells, as reported by Hauch et al.[12] Aging is produced in part due to nickel coarsening in the fuel electrode but is also mainly due to the ion migration from the sealing glasses. The use of microtubular cells are proposed as an alternative to solve this problem, as high temperature seals are not required in the microtubular design.

Microtubular SOFCs have attracted some interest in recent years.[13,14] Those devices are envisaged for mobile applications in opposition to polymer electrolyte fuel cell devices.[15] The major advantages of the microtubular SOFC, mainly in comparison with the planar design but also with conventional tubular cells, are high thermal shock resistance and short times to startup and shutdown (rapid thermal cycling) and less redox cycling damage. Moreover, high power densities per unit volume are achieved by reducing the diameter of the tubes. In this paper, we report on an efficient micro-SOFC cell in both modes of operation. These microtubular SOFC devices present good properties for steam electrolyzers as they are able to support both high heating–cooling rates and high current densities for a small cell volume. Recently, Hashimoto et al. reported a microtubular SOE based on the scandia-stabilized zirconia electrolyte.[16] They have measured a voltage of 1.37 V using 18% $H_2O$/10% $H_2$/72% Ar as a fuel at $-0.1$ A/cm$^2$ and 700°C with an area-specific resistance (ASR) of 4.3 Ω cm$^2$. They suggest that the activation polarization is the major effect for the potential drop in the steam electrolysis possibly due to a contact problem between the Lantanum strontium cobalt ferrite (LSCF) and the electrolyte. Although they have achieved a modest cell performance, they have demonstrated for the first time that microtubular cells are good candidates for steam electrolyzers.

* Electrochemical Society Active Member.
z E-mail: malaguna@unizar.es

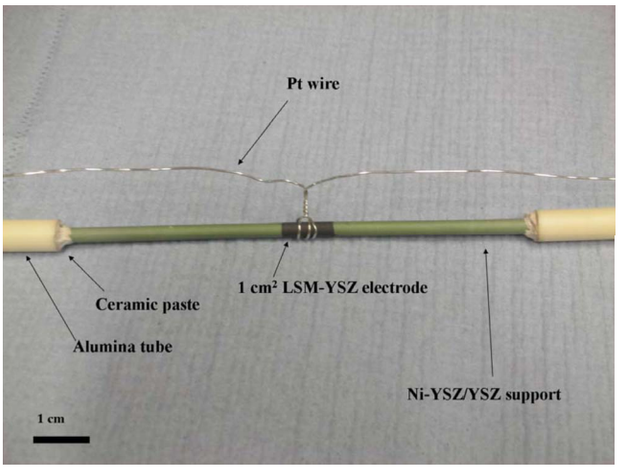


(a)

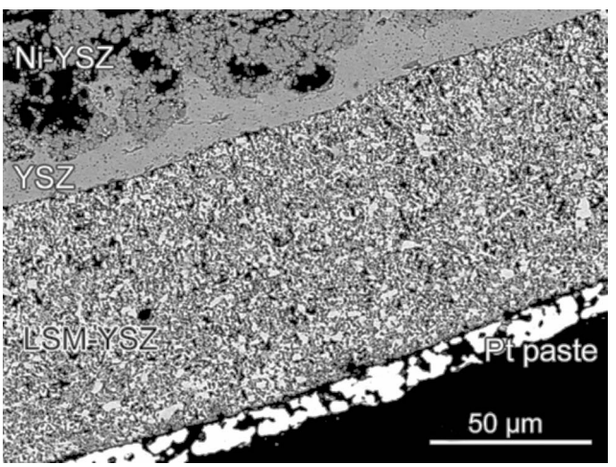


(b)

**Figure 1.** (Color online) (a) Image of the microtubular cell (before reduction) showing the electric connections at the anode. (b) Backscattered SEM micrograph (polished cross section) showing the microstructure of the anode supported Ni/YSZ/YSZ–LSM/YSZ cell.

## Experimental

The cell configuration used for the electrochemical experiments consisted of a microtube of nickel/yttria-stabilized zirconia (Ni/YSZ) cermet of 10–15 cm length and 2.4 mm inner diameter fabricated by a cold isostatic pressing at 200 MPa. The YSZ gastight electrolyte was then deposited by wet powder spraying using 2-propanol as the liquid vehicle. The Ni/YSZ electrode–YSZ electrolyte were cosintered at 1400°C. Finally, A-site deficient manganite $[(La_{0.8}Sr_{0.2})_{0.98}MnO_3]$ (LSM)/YSZ (50/50 wt %) composite air electrodes were deposited by dip-coating and were sintered at 1250°C. The fabrication procedure and the composition of the components were tailored to obtain optimum gas and electronic transport, as well as a good thermomechanical stability, as described by Campana et al.[17]

SOFC–SOEC experiments were performed at temperatures between 750 and 950°C using different partial pressures of steam in the inner side (Ni/YSZ) and synthetic air for the oxygen electrode side. Steam was supplied to the cathode by the use of a gas bubbler in water surrounded by a thermostatic bath, maintained at a constant temperature for the required amount of steam with the steam content measured using a humidity sensor (the resolution was ±5%). All gas lines located downstream of the humidifier were externally heated to prevent steam condensation. The outlet gas was then cooled to get high quality mass spectrometry data, avoiding water condensation. The experimental setup was similar to that explained in Ref. 18 for the planar single cells. Pt wires were used for the current injection and potential probe, and the Ni foam (for the Ni/YSZ cathode) and Pt paste (for the LSM/YSZ anode) were used as current collectors. The active area used for the experiments is ~1 $cm^2$, as shown in Fig. 1a. Microtubular cells were then sealed into alumina tubes on both sides using a ceramic paste to facilitate gas connections. The temperatures stated in the text correspond to cell temperatures. For that purpose, an external thermocouple was placed close to the oxygen electrode active area of the cell. Galvanostatic and galvanodynamic experiments were performed using an Autolab PGSTAT30. All the scan directions of the voltage–current (*V-I*) curves presented in the text start from the open-circuit voltage (OCV). The scan rate in all the galvanodynamic experiments was 2.5 mA $cm^{-2}$ $s^{-1}$. The scanning electron microscopy (SEM) experiments were performed under an accelerating voltage of 15 kV using a JEOL 6400 SEM fitted with Oxford Instruments INCA energy dispersive analytical system for the elemental X-ray analysis.

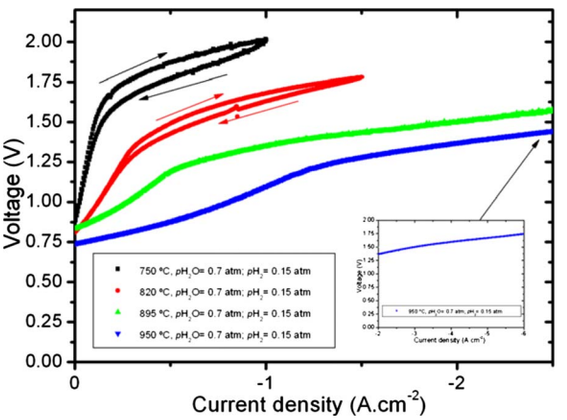


**Figure 2.** (Color online) *V-I* curves in electrolysis mode performed as a function of the temperature and a partial pressure of steam supplied to the Ni/YSZ side of the cell of $pH_2O = 0.7$ atm. Direction of the reverse scans are shown at 750 and 820°C.

## Results and Discussion

The structure of the cell is shown in Fig. 1a, and the microstructure of the cell components and their interfaces are shown in Fig. 1b. The thicknesses of the different components are ~350–400 µm for the NiO/YSZ support, 15–20 µm for the thin YSZ electrolyte layer, and ~60–80 µm for the LSM/YSZ oxygen electrode. The anode has an open porosity of around 40%, and the particle size of Ni and YSZ are almost identical (about 0.8–1 µm), ensuring good microstructure homogeneity and permeability, essential for a high number of triple-phase boundaries. The anode–electrolyte interface shows a tree-root structure, and the electrolyte layer is tight to gas permeation.

In Fig. 2, we present results as a function of the temperature for SOEC experiments performed at 70% steam concentration. As expected, smaller slopes are obtained when increasing the temperature. The activation polarization is not observed at low current densities. This is also confirmed by the reverse scans showed in Fig. 2 for the lower temperatures. From those reverse scans, we observed that the *V-I* data are quasi-stationary at low current densities. However, at current densities above ~0.5 A/$cm^2$, a nonreversible behavior was observed. The LSM electrode presents an activation under high current densities, as previously reported for example in Refs. [19,20]. If we apply a fixed current through the cell before the electrolysis experiments, the nonreversible behavior observed at 750 and 820°C

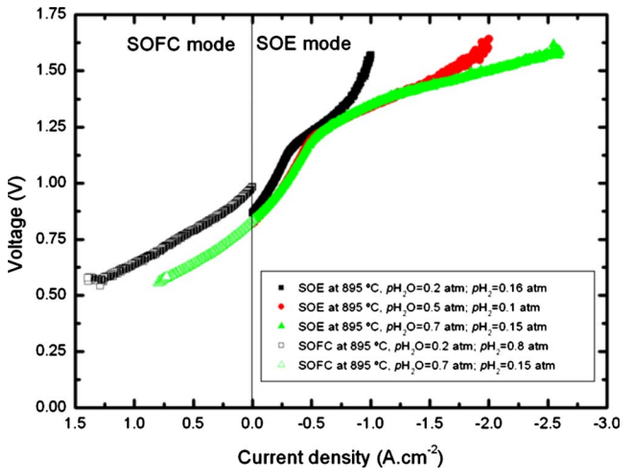


**Figure 3.** (Color online) *V-I* curves in electrolysis and fuel cell mode at 895°C for the microtubular cell under different conditions. The SOFC–SOE curves for 25% steam concentration do not fit because of the different $H_2$ partial pressures.

is clearly reduced, and the *V-I* behavior is stabilized to a stationary state similar to the reverse scans. The *V-I* curves at 895 and 950°C showed in Fig. 2 correspond to a stationary state.

The *V-I* curves present an S-shaped behavior, as observed in Fig. 2. At intermediate current densities (between ~0.5 and ~1 $A/cm^2$), the slope starts to decrease dramatically. The total ASRs of the cells (obtained from OCV to 1.5 V) are 2.58, 1.21, 0.32, and 0.26 $\Omega\ cm^2$ at 750, 820, 895, and 950°C, respectively. It is also clearly observed in the graph that lower ASRs could be obtained from the high current density regions. For example, at 895°C, an ASR of 0.16 $\Omega\ cm^2$ is obtained from the slope in the exothermic region (from 1.3 to 1.58 V). In the electrolysis mode, increasing the temperature up to 950°C, we have obtained a current density of $-2.95\ A/cm^2$ using 70% $H_2O$/15% $H_2$/15% $N_2$ as a fuel at 1.5 V, with a total internal resistance of 0.26 $\Omega\ cm^2$ (measured from OCV to 1.5 V). At this temperature, the cell was also able to support high current densities of about $-6\ A/cm^2$ without apparent cell damage. The internal resistance of the cell at high voltage values (above 1.3 V) is as low as 0.10 $\Omega\ cm^2$.

The production of hydrogen in the electrolyzer at moderate current densities was also confirmed by mass spectrometry. For this purpose, galvanostatic measurements were carried out at 850°C and a fixed current density of $-1\ A/cm^2$. The inlet gas was 70% $H_2O$/15% $H_2$/15% $N_2$ ($Q_T$ = 60 mL/min) with a steam utilization of 16.5%. Under these conditions, the measured hydrogen after water condensation was ~97% that of the theoretical (faradaic efficiency), confirming the high current efficiency for the steam electrolysis. The results at 895°C as a function of the steam concentration (20 and 70%) in the electrolysis and fuel cell mode are presented in Fig. 3, where the reversible behavior of the cell can be appreciated. The OCV values agree well with the obtained values using the Nernst equation for the different steam concentrations. The concentration polarization is also clearly observed in Fig. 3 for low steam concentration at high current densities that corresponds with the steam utilization of about 40%, a high conversion value for the small active area of the cell (1 $cm^2$). As we increase the concentration of steam in the cathode, the performance of the cell is clearly enhanced.

At this temperature, where the electronic properties of the LSM/YSZ anode are optimal, the cell displays good electrochemical performance in both modes of operation. As we can observe in the figure, the cell is reversible under 70% of steam at 895°C. Under the SOFC mode, ASR values are similar for different steam concentrations under pure hydrogen. Small differences could be associated to the concentration polarization resulting from the gas diffusion through the porous anode due to the different steam concentration. For example, at 895°C, the maximum power densities of 800, 650, and 440 mW $cm^{-2}$ for 3, 25, and 70% $H_2O$, respectively, were obtained under the SOFC mode.

As pointed out before, there is a saturation of the cell voltage at high current densities in the electrolysis mode at voltages around 1.3 V. As a consequence, the cell can support very high current densities up to $-6\ A/cm^2$, which was our experimental limit. The theoretical steam utilization at $-6\ A/cm^2$ would be higher than 100%, which is not possible, and also, we should obtain a notable concentration polarization that we do not observe.

The origin of this effect is still unclear, and two possible explanations are proposed. The first explanation would be drawn from the Joule heating effect due to the thermodynamics of the steam electrolysis reaction. In fact, when the voltage is higher than the thermoneutral voltage (~1.3 V), the Joule heat produced within the cell cannot be efficiently dissipated and the temperature of the cell increases. As a consequence, the cell resistance decreases not only because the electrolyte ohmic resistance decreases, but also because the electrical conductivity of the LSM electrode increases. Even though an accurate measurement of the cell temperature is difficult due to the space in the location of the external thermocouple, an increase of as much as 30–40°C on the cell temperature has been recorded during the exothermic operation at the highest current values. Clearly, this rise in temperature could only partially account for the observed behavior.

Another explanation for this effect is the existence of electronic conductivity in the YSZ electrolyte, which would drop the cell impedance, enabling higher currents. Electrolyte shorts due to the electrolyte reduction have also been reported as a matter of concern of electrolysis cells.[21] Similar *V-I* curve shapes were recently observed by Schefold et al.[22] in anode-supported planar SOECs. These authors argue in favor of an electronic short-circuit on the thin electrolyte. The effect appears at voltages lower than the YSZ reduction potential of about 2.3 V [23] and might be caused by the YSZ decomposition. They have also reported that this electronic conduction can prevent an electrolyte damage when the steam supply is interrupted, as they survive a long-term galvanostatic operation without a steam supply.

The authors believe that a similar behavior could be occurring in their case, although different cells are under study to understand the process in detail and also to avoid the YSZ electroreduction.

Finally, we remark on the apparently excellent performance of the electrodes in the SOEC mode. Ni/YSZ cermets are expected to perform well as a cathode for SOEC, as nickel is an excellent catalyst for the water reduction reaction (Eq. 2). On the contrary, the performance of LSM as an oxygen evolution electrode (Eq. 3) is uncertain as it is a pure electronic conductor. Some previous work has demonstrated that perovskite-based SOFC cathodes on YSZ electrolytes present an improvement on their performance under polarization.[19,20] Under high current densities, the contribution of the charge-transfer resistance is strongly reduced. Recently, Backhaus-Ricoult et al.[24] studied the surface chemistry of LSM/YSZ composites under polarization. They observed that there is a strong enrichment of the YSZ surface in $Mn^{2+}$ that provides high electronic conductivity in the zirconia surface region and promotes the direct incorporation of oxygen from the gas into the electrolyte. A similar mechanism could occur in the electrolysis mode for the oxygen evolution, explaining the good performance of the LSM/YSZ as an SOEC anode.

## Conclusions

Highly efficient reversible microtubular cells are presented in this paper. At 895°C, a maximum power density of 800 mW $cm^{-2}$ was obtained under the SOFC mode. In the electrolysis mode, we have operated the cell at current densities of $-1\ A/cm^2$ using 70% $H_2O$/15% $H_2$/15% $N_2$ as a fuel at 1.3 V and 850°C.

At higher voltages, the cell resistance drops and high current

densities can be supported by the cell. At high current densities, the electronic conduction of the YSZ electrolyte, which suffers electroreduction processes, is suggested to be, from indirect experimental evidence, the reason for this reversible effect. We have demonstrated that these microtubular cells are very efficient and reversible, and especially their performance in the SOE mode is very promising for high temperature electrolysis applications, as confirmed at moderate current densities by mass spectrometry measurements.

## Acknowledgments

The authors thank UKERC (NERC-TSEC program grant no. NE/C516169/1) and grants MAT2009-14324-C02-01, GA-LC-009/2009, and CIT-120000-2007-50 financed by the Spanish government, and DGA-Caixa and Feder program of the European Community for funding the project. R.C. and M.A.L.-B. also thank IKERLAN-Energía and the JAE-program (CSIC) for financial support.

*Universidad de Zaragoza assisted in meeting the publication costs of this article.*

## References

1. E. W. Dönitz and E. Erdle, *Int. J. Hydrogen Energy*, **10**, 291 (1985).
2. S. H. Jensen, P. H. Larsen, and M. Mogensen, *Int. J. Hydrogen Energy*, **32**, 3253 (2007).
3. S. D. Ebbesen and M. Mogensen, *J. Power Sources*, **193**, 349 (2009).
4. I. Chorkendorff and J. W. Niemantsverdriet, *Concepts of Modern Catalysis and Kinetics*, Wiley-VCH, Weinheim (2006).
5. W. Wang, J. M. Vohs, and R. J. Gorte, *Top. Catal.*, **46**, 380 (2007).
6. J. Martinez-Frias, A. Q. Pham, and S. M. Aceves, *Int. J. Hydrogen Energy*, **28**, 483 (2003).
7. W. Wang, Y. Huang, S. Jung, J. M. Vohs, and R. J. Gorte, *J. Electrochem. Soc.*, **153**, A2066 (2006).
8. O. A. Marina, L. R. Pederson, M. C. Williams, G. W. Coffey, K. D. Meinhardt, C. D. Nguyen, and E. C. Thomsen, *J. Electrochem. Soc.*, **154**, B452 (2007).
9. G. Schiller, A. Ansar, M. Lang, and O. Patz, *J. Appl. Electrochem.*, **39**, 293 (2009).
10. A. Brisse, J. Schefold, and M. Zahid, *Int. J. Hydrogen Energy*, **33**, 5375 (2008).
11. A. Hauch, S. D. Ebbesen, S. H. Jensen, and M. Mogensen, *J. Mater. Chem.*, **18**, 2331 (2008).
12. A. Hauch, S. D. Ebbesen, S. H. Jensen, and M. Mogensen, *J. Electrochem. Soc.*, **155**, B1184 (2008).
13. N. M. Sammes, R. J. Boersma, and G. A. Tompsett, *Solid State Ionics*, **135**, 487 (2000).
14. G. A. Tompsett, C. Finnerty, K. Kendall, T. Alston, and N. M. Sammes, *J. Power Sources*, **86**, 376 (2000).
15. K. Kendall, *Int. J. Appl. Ceram. Technol.*, **7**, 1 (2009).
16. S. Hashimoto, Y. Liu, M. Mori, Y. Funahashi, and Y. Fujishiro, *Int. J. Hydrogen Energy*, **34**, 1159 (2009).
17. R. Campana, R. I. Merino, A. Larrea, I. Villarreal, and V. M. Orera, *J. Power Sources*, **192**, 120 (2009).
18. M. A. Laguna-Bercero, J. A. Kilner, and S. J. Skinner, *Chem. Mater.*, **22**, 1134 (2010).
19. S. P. Jiang and L. G. Love, *Solid State Ionics*, **158**, 45 (2003).
20. S. Adler, *Chem. Rev. (Washington, D.C.)*, **104**, 4791 (2004).
21. A. O. Isenberg, *Solid State Ionics*, **3–4**, 431 (1981).
22. J. Schefold, A. Brisse, and M. Zahid, *J. Electrochem. Soc.*, **156**, B897 (2009).
23. W. Weppner, *J. Electroanal. Chem. Interfacial Electrochem.*, **84**, 339 (1977).
24. M. Backhaus-Ricoult, K. Adib, T. St. Clair, B. Luerssern, L. Gregoratti, and A. Barinov, *Solid State Ionics*, **179**, 891 (2008).